

# Maleated Polyisobutylene: A Novel Toughener for Unsaturated Polyester Resins

M. ABBATE, E. MARTUSCELLI, P. MUSTO, G. RAGOSTA,\* and G. SCARINZI

National Research Council of Italy, Institute of Research and Technology of Plastic Materials, via Toiano, 6, 80072 Arco Felice, Naples, Italy

## SYNOPSIS

A polyisobutene rubber was modified by grafting succinic anhydride onto its end groups and has been used as a toughening agent for an unsaturated polyester resin. Both the functionalization and the successive reaction between the modified rubber and the polyester was investigated by Fourier transform infrared spectroscopy (FTIR). The yield behavior of the cured resins was studied by compression measurements, while the fracture properties were determined at low and high strain rate. A morphological analysis of the investigated blends has been carried out by scanning electron microscopy (SEM). A considerable enhancement of toughness has been achieved when the modified rubber was used in place of the plain polyisobutene. The effect was found to depend on the grafting degree of the rubber and on the time period during which the two-component mixture was allowed to react prior to the curing process. © 1995 John Wiley & Sons, Inc.

## INTRODUCTION

Unsaturated polyesters (UP) are used extensively as matrices in fiber-reinforced composite systems. They are particularly useful in sheet-molding compounds (SMC) and bulk-molding compounds (BMC) for manufacturing automotive parts.

Common commercial resins are available in the form of relatively low molecular weight linear polyesters in solution with a reactive monomer which is generally styrene. They are crosslinked by a radical mechanism through an addition copolymerization with the monomer. The polyester prepolymer is prepared by a condensation reaction of a glycol such as ethylene or propylene glycol and an unsaturated anhydride or dibasic acid such as maleic anhydride. Because a wide variety of acids or anhydrides can be substituted in the polymer backbone, different base resins are available which exhibit a broad spectrum of performance characteristics.

However, the whole family of UP resins suffer a

major drawback, namely, their brittleness and poor resistance to crack propagation.<sup>1,2</sup> This limitation has confined the application of UPs to situations where the stress is relatively low and preferably static. In the case of other thermosets, such as epoxies, this problem has been solved by blending with reactive liquid rubbers.<sup>3-5</sup> This technique has had limited success in the case of UP resins because of the poor solubility of the rubber component in the unreacted resin and of the low chemical reactivity of the rubber toward the polyester end group.<sup>6</sup> Efforts to chemically modify commercial liquid rubbers to enhance their reactivity toward the UP matrix are underway in our institute. In particular, in a previous contribution,<sup>7</sup> a hydroxyl-terminated polybutadiene was transformed into an isocyanate-terminated rubber and the isocyanate functionalities were reacted with the hydroxyl end groups of the UP resin prior to the curing process. In the present work, a further modification of a commercial liquid rubber is described: A polyisobutylene (PIB) having an olefinic end group was reacted with maleic anhydride to obtain PIB bearing anhydride functionalities (PIBSA). These anhydride groups are able to react with the hydroxyl end

\* To whom correspondence should be addressed.

groups of the UP chains, forming a block copolymer UP/PIB which can act as an emulsifier in a UP/PIB blend.

The molecular characterization of such a modified rubber was accomplished by Fourier transform infrared spectroscopy (FTIR). The same spectroscopic technique was used to investigate in detail the reaction between PIBSA and the UP matrix. The mechanical and the fracture properties of the cured materials were studied at low and high rates of deformation using the linear elastic fracture mechanics approach. The results of such an analysis were correlated eventually with the morphology of the samples investigated by SEM and image analysis.

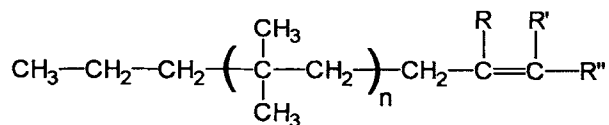
## EXPERIMENTAL

### Materials

The UP resin was an uncured, unsaturated polyester kindly supplied by Alusuisse Italia. The resin was available either as a solution containing 35% of styrene or in the form of the pure prepolymer. The acid number of the prepolymer, defined as the mg of KOH used for the titration of 1 g of prepolymer, was 19.2.

The OH number, obtained by titration of the excess acetic anhydride used to fully esterify the hydroxyl groups, was 53.4. This corresponds to 0.34 mmol of COOH groups and 0.95 mmol of OH groups per gram of resin. In the UP formulation, 0.1% by weight of hydroquinone was employed as inhibitor to prevent premature curing. Benzoyl peroxide (BPO) was the radical initiator and was recrystallized twice from absolute ethanol before use.

The liquid rubber was a polyisobutylene (PIB) supplied by BP Chemicals having a molecular weight,  $\bar{M}_n = 2400$ . Its chemical formula is reported below:



PIB

where R, R', R'' = H, CH<sub>3</sub>

The technical note provided by the producer states that PIB has a double bond per chain in the end group, as determined by NMR spectroscopy. This double bond can be either di- or trisubstituted, while tetrasubstituted unsaturations were excluded by UV analysis; moreover, the disubstituted double bonds can be of the vinyl or vinylidene type.

### Preparation of Polyisobutylene-grafted Succinic Anhydride (PIBSA)

In a three-necked round-bottom flask equipped with a nitrogen inlet, 20 g of PIB was dissolved by refluxing in 400 mL of toluene under magnetic stirring. The solution was heated to 120°C and 4 g of maleic anhydride (MA) was added through a funnel. Upon complete dissolution, a solution of BPO (2 g) in 20 mL of toluene was added. The solution was refluxed under nitrogen atmosphere and magnetic stirring for 3 h.

After cooling, the solvent was removed under vacuum and the residue was dissolved in *n*-hexane in which the rubber is soluble while MA is not. The resulting solution was separated by centrifugation, then filtered through a sintered glass to remove the traces of byproduct and the excess of MA. Hexane was then evaporated from the filtrate, leaving a clear thick viscous liquid. This product was finally dried in a vacuum oven for 16 h at 60°C. The previous procedure was used to prepare another sample of PIBSA with a grafting degree of 2.5% by weight; in this case, 20 g of PIB, 23 g of MA, and 6 g of BPO initiator were used.

### Preparation of a Typical UP/Rubber Blend

Seven grams of rubber PIBSA were put in a reaction vessel with 63 g of UP resin and styrene monomer in the ratio 65/35 w/w. The mixing was continued for 1 h at 60°C, under vigorous mechanical stirring.

After the homogenization of the mixture, the temperature was allowed to decrease to 20°C and 1.26 g of BPO were added, continuing the mixing for an additional 10 min. At this stage, the mixture was poured in a glass mold which was immediately immersed in a thermostatic bath kept at 50°C for 2 h. The cure was continued for 10 h at 70°C and was followed by a postcure at 100°C for 2 h. The investigated blend compositions with their codes are reported in Table 1.

**Table I** Codes and Compositions of the UP/Rubber Blends

Code	UP (%)	PIB (%)	PIB GD (%)
UP	100	—	—
B0	90	10	—
B1.5	90	10	1.5
B2.5	90	10	2.5
B2.5 <sup>a</sup>	90	10	2.5

<sup>a</sup> Premixed 12 h before curing.

## Techniques

FTIR spectra were obtained at  $2\text{ cm}^{-1}$  resolution with a Perkin-Elmer System 2000 spectrometer equipped with a deuterated triglycine sulfate detector (DTGS) and a germanium/KBr beam splitter. The recorded wavenumber range was  $4000\text{--}4501\text{ cm}^{-1}$  and 30 spectra were signal-averaged in the conventional manner to reduce the noise. The measurements were carried out either on thin ( $1\text{--}5\text{ }\mu\text{m}$ ) films cast on KBr disks from  $\text{CH}_2\text{Cl}_2$  or as solutions in  $\text{CH}_2\text{Cl}_2$ . In all cases, the film thickness or the liquid cell thickness were chosen so as to keep the absorbance of the region of interest in a range where the Beer-Lambert law is obeyed.

Uniaxial compressive tests were made on parallelepipedal samples 12 mm long, 6.0 mm wide, and 4.0 mm thick using an Instron mechanical tester at ambient and at a crosshead speed of 1 mm/min. Three-point bending specimens were used to perform fracture tests at room temperature and at low and high strain rate.

The low strain rate measurements were carried out on an Instron apparatus at a crosshead speed of 1 mm/min. The high strain rate tests were performed on a Charpy instrumented pendulum at an impact speed of 1 m/s. For both, the tests samples ( $60 \times 6.0 \times 4.0\text{ mm}$ ) were cut from sheets of the cured materials and then sharply notched. The fracture data were analyzed according to the concepts of linear elastic fracture mechanics.<sup>8</sup>

The critical stress intensity factor,  $K_c$ , was calculated by means of the equation

$$K_c = \sigma Y \sqrt{a} \quad (1)$$

where  $\sigma$  is the nominal stress at the onset of crack propagation;  $a$ , the initial crack length; and  $Y$ , a calibration factor depending upon the specimen geometry. For three-point bending specimens,  $Y$  is given by Brown and Srawely.<sup>9</sup> For the determination of the critical strain energy rate,  $G_c$ , the following equation was used:

$$G_c = \frac{U}{BW\Phi} \quad (2)$$

where  $U$  is the fracture energy;  $B$  and  $W$ , the thickness and the width of the specimen, respectively; and  $\Phi$ , a calibration factor which depends on the length of the notch and the size of the sample. Values of  $\Phi$  were taken from Plati and Williams.<sup>10</sup>

Fractured surfaces were coated with a thin layer of a gold-palladium alloy and then examined by

SEM. Prior to SEM examination, some samples were etched with boiling  $\text{CHCl}_3$  to selectively remove the rubber component. The size and distribution of the rubber particles within the UP matrix were determined from SEM micrographs of etched surfaces using image analysis. The Quantimet 900 image analysis system was used for this purpose.

## RESULTS AND DISCUSSION

### FTIR Analysis

In Figure 1 are compared the FTIR spectra in the frequency range  $4000\text{--}450\text{ cm}^{-1}$  of the plain rubber (curve A) and of a PIBSA sample having a grafting degree of 1.5% wt/wt (curve B). The peaks arising from the vibrations of the grafted succinic anhydride groups are found in the curve B of Figure 1 at 1860, 1783, 1716, and  $701\text{ cm}^{-1}$  (Ref. 11). In particular, the doublet at  $1860\text{--}1783\text{ cm}^{-1}$  is due to the in-phase and out-of-phase vibrations of the anhydride carbonyls, while the  $1716\text{ cm}^{-1}$  component arises from the  $\nu_{\text{C=O}}$  vibration of the succinic acid. Its presence indicates that a very limited amount of anhydride underwent hydrolysis. The carbonyl region is free from interfering PIB absorptions and the peak at  $1782\text{ cm}^{-1}$  has been used to quantitatively evaluate the amount of SA bound on the PIB backbone.

The quantitative determination has been performed on solutions of PIBSA in  $\text{CH}_2\text{Cl}_2$  by means of the calibration curve reported in Figure 2. This curve was constructed using succinic anhydride solutions in  $\text{CH}_2\text{Cl}_2$  as standards. The two PIBSA samples prepared according to the procedure reported in the Experimental section yielded a grafting degree of 1.5 and 2.5% wt/wt, respectively.

There are several studies dealing with the grafting of MA and other reactive monomers onto saturated and unsaturated rubbers, initiated by organic peroxides. In the case of saturated rubbers, it has been shown that the grafting occurs preferentially onto the methylene groups and, in particular, onto the longer and more regular  $\text{---CH}_2\text{---}$  sequences.<sup>12,13</sup> For unsaturated elastomers such as polyisoprene or polybutadiene,<sup>14</sup> the MA addition occurs in the vicinity of the double bond and preferentially in the  $\alpha$  position with respect to the unsaturation.

In our case, we used FTIR spectroscopy to establish the preferential site of addition along the PIB chain. It is well known that vinyl groups give rise to a medium-intensity absorption in the range  $900\text{--}890\text{ cm}^{-1}$  due to an out-of-plane deformation mode of the group. This peak goes completely un-

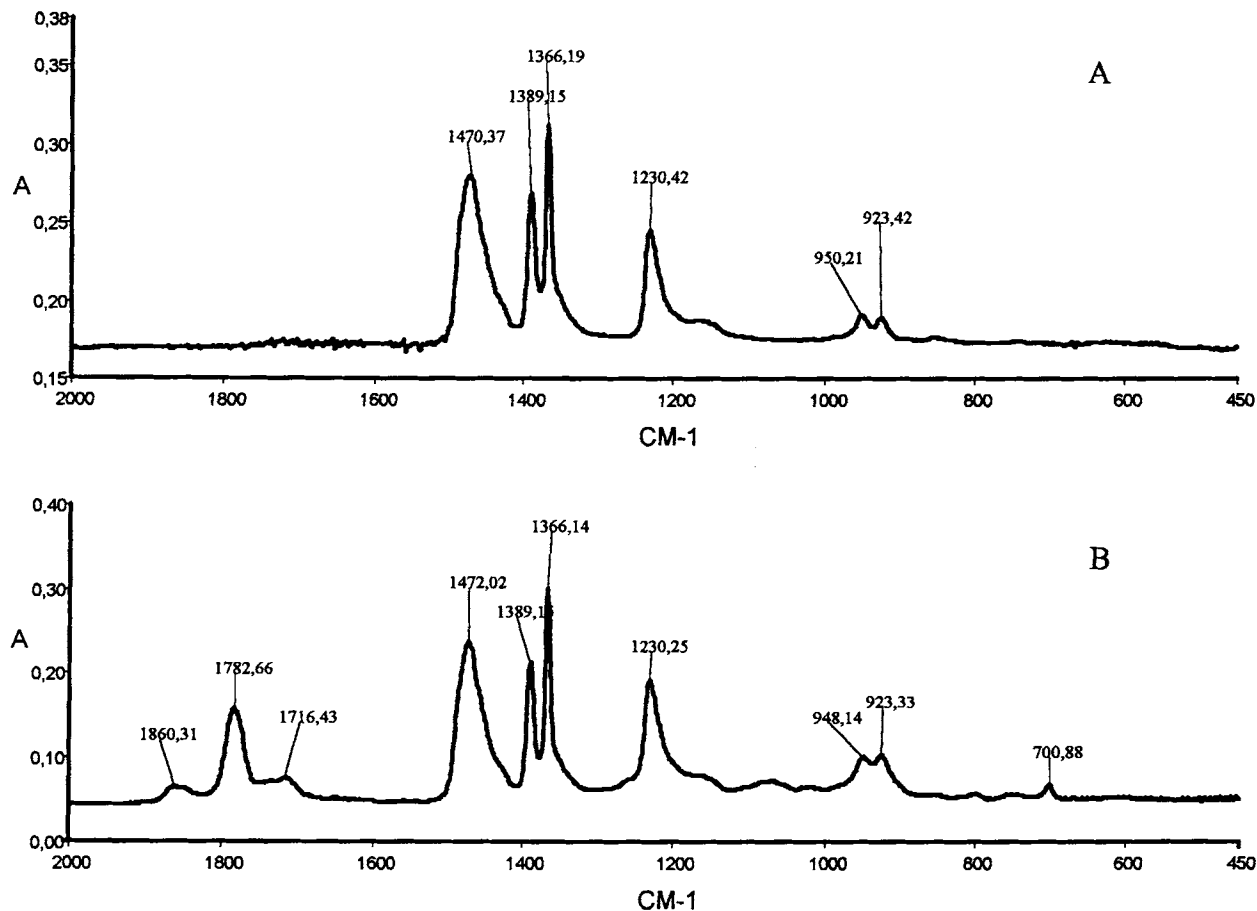


**Figure 1** FTIR spectra in the frequency range 4000–450 cm<sup>-1</sup> of (curve A) plain PIB and of (curve B) PIBSA with a GD of 1.5% wt.

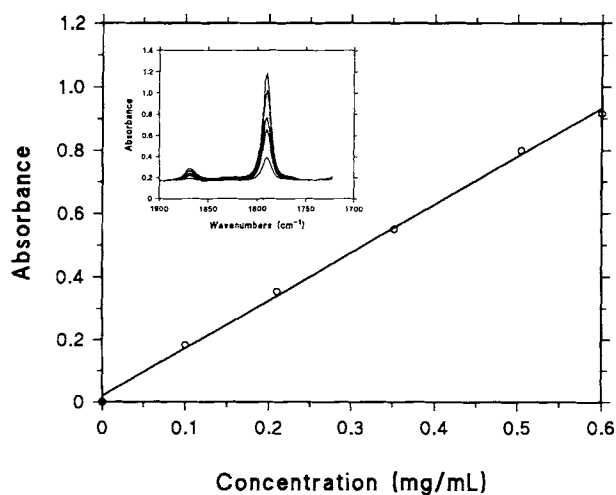


**Figure 2** Calibration curve for the quantitative determination of the grafting degree. The inset displays the peaks used for the construction of the curve.

detected in the spectrum of a thin PIB film [see Fig. 1(A)] due to the very low concentration of the vinyl end groups into the PIB sample. However, increasing the sample thickness from few microns up to 0.5 mm, a well-resolved absorption is detected in the expected frequency range [see Fig. 3(A)].

To confirm the assignment of such a peak to a wagging mode of the vinyl groups, halogenation of the PIB end groups was performed; the spectral profile of the fully iodinated PIB, reported in Figure 3(B) in the frequency range 900–780 cm<sup>-1</sup>, shows the complete disappearance of the peak at 891 cm<sup>-1</sup>, thus confirming the assignment. The spectrum of the PIBSA sample having a grafting degree of 2.5 is reported in Figure 3(C). Also, in this case, the component at 891 cm<sup>-1</sup> is absent, which indicates that all the vinyl end groups have reacted with MA.

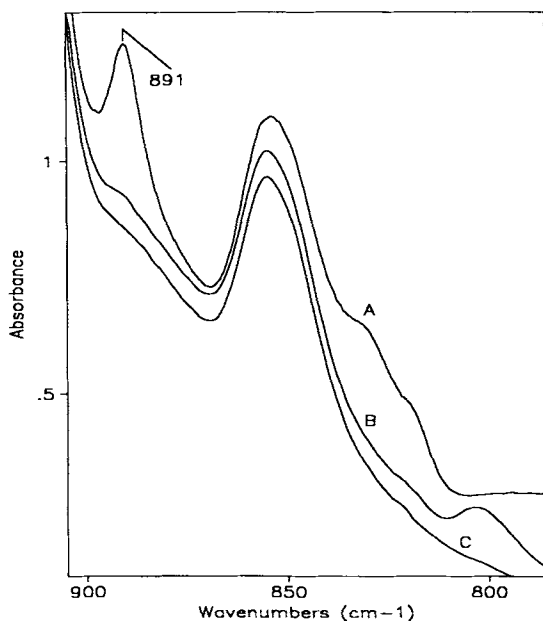
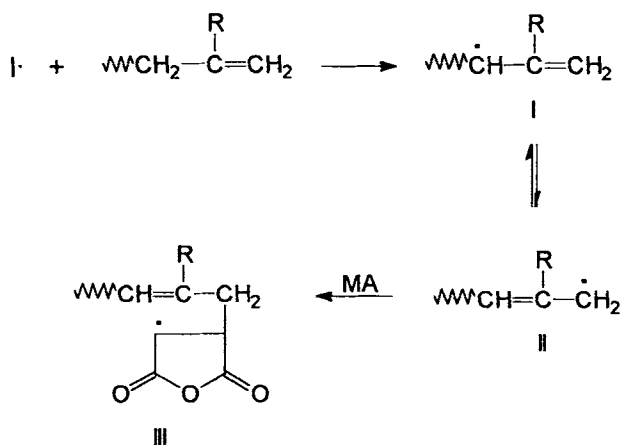
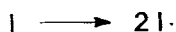


**Figure 3** FTIR spectra in the frequency range 900–780  $\text{cm}^{-1}$  of (curve A) plain PIB, (curve B) fully iodinated PIB, and (curve C) PIBSA having a GD of 2.5. The spectra were collected on films 0.5 mm thick.

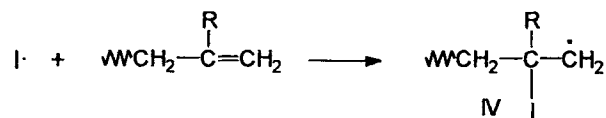
On this basis, the following reaction mechanism may be assumed:



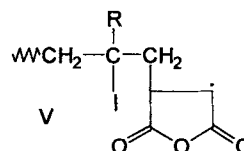
Structure **III** may either interact with a PIB molecule, to yield PIBSA and structure **I** by a chain propagation step, or may terminate by coupling or disproportionation with another radical species.

A further possibility also cited in the literature,<sup>15</sup> but, in our opinion, less likely to occur, involves as

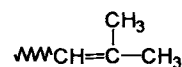
the first step the direct addition of the primary radical  $I \cdot$  onto the double bond:



Structure **IV** will then add an MA molecule to form

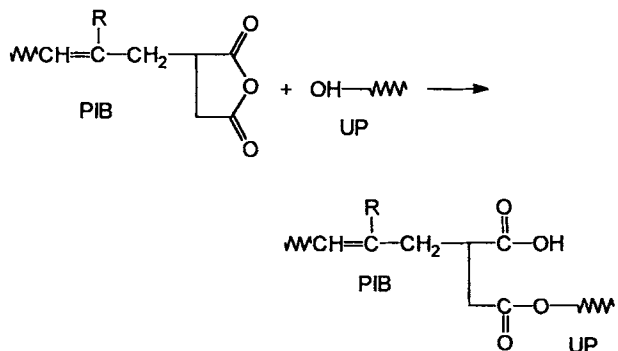


which, in turn, will evolve in the same way as structure **III**. It is noted that the total concentration of double bonds in PIB is 0.405 mmol/g and that the maximum concentration of grafted MA, corresponding to a grafting degree of 2.5% wt/wt, is 0.265 mmol/g. Attempts to increase the grafting degree by varying the reaction conditions (temperature, peroxide, and MA concentration) were unsuccessful. Thus, only about 65% of the total amount of terminal double bonds of PIB are reactive toward MA addition. The remaining 35% of unreactive double bonds may be assumed to be of the trisubstituted type:



and their lower reactivity could be ascribed to steric effects.

When PIBSA is mixed with UP, the following esterification reaction may occur:



which would yield a diblock copolymer of the type PIB/UP. The process has been investigated by

FTIR spectroscopy: The PIBSA/UP reaction mixture was held at 80°C under vigorous mechanical stirring. At various time intervals, different aliquots were withdrawn and analyzed spectroscopically as solution in CH<sub>2</sub>Cl<sub>2</sub>.

Using the appropriate concentration range, the succinic anhydride doublet is clearly discerned as a low intensity peak centered at 1860 cm<sup>-1</sup> and as a well-defined shoulder at 1783 cm<sup>-1</sup> of the ν<sub>C=O</sub> mode of the polyester (see Fig. 4). Figure 4 also shows that the intensity of the ν<sub>as,C=O</sub> peak of the grafted anhydride decreases gradually by increasing the reaction time.

To obtain more quantitative information, the spectral data of Figure 4 were analyzed by difference spectroscopy. A pseudo-base line was identified in the frequency range 1873–1763 cm<sup>-1</sup> as the spectral profile of the neat UP resin (Fig. 4, curve A). Subtraction of such a base line from the spectra of Figure 4 allowed us to eliminate the interference of the ν<sub>C=O</sub> absorption of the UP carbonyls so as to obtain a fully resolved profile of the anhydride doublet (see Fig. 5). The percent anhydride conversion was then evaluated from the intensity of the ν<sub>C=O</sub> peak at 1783 cm<sup>-1</sup> as

$$\alpha(t) = \frac{100\{[SA]_0 - [SA]_t\}}{[SA]_0} = 100 \left\{ 1 - \frac{[SA]_t}{[SA]_0} \right\} \quad (3)$$

$$\alpha(t) = 100 \left\{ 1 - \frac{A_t C_0}{A_0 C_t} \right\} \quad (4)$$

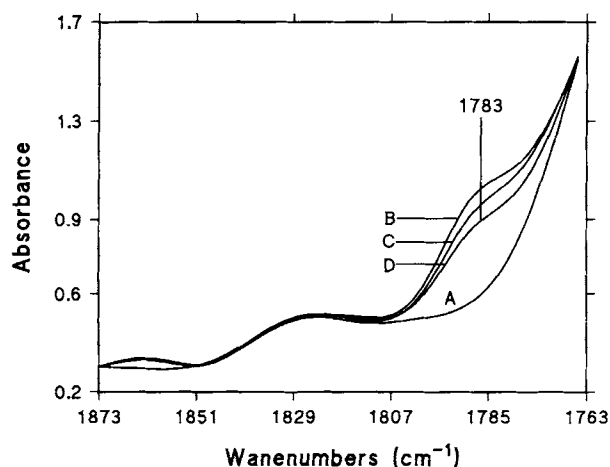


**Figure 4** FTIR solution spectra in the frequency range 1873–1763 cm<sup>-1</sup> of (curve A) the plain UP resin and of (curves B, C, and D) a B2.5 blend. Traces B, C, and D refer to premixing times of 0, 215, and 800 min, respectively.

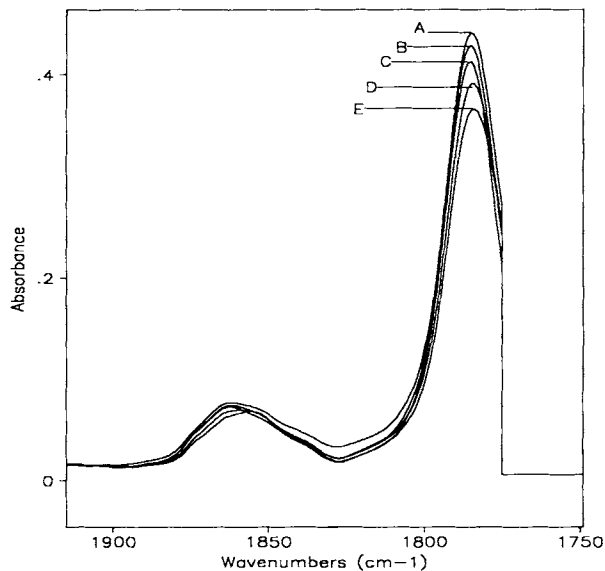


**Figure 5** Subtraction analysis in the frequency range 1920–1750 cm<sup>-1</sup> of the solution spectra of the B2.5 blend. Curves A, B, C, D, and E refer to premixing times of 0, 90, 215, 335, and 800 min, respectively.

where [SA] is the concentration of succinic anhydride groups in the reactive mixture, *C* is the concentration of the reactive mixture in the CH<sub>2</sub>Cl<sub>2</sub> analytical solution, and the subscripts 0 and *t* refer to reaction times 0 and *t*, respectively.

The results of this analysis are reported in Figure 6. It is immediately apparent that the maximum attainable conversion is about 15%; the reaction proceeds at an almost constant rate of 0.034 min<sup>-1</sup> up

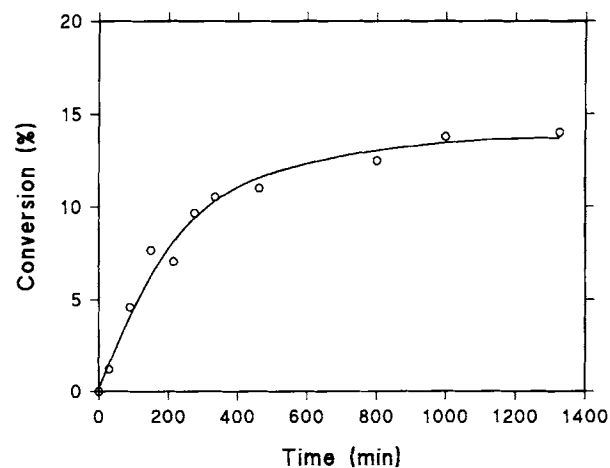


**Figure 6** Conversion of anhydride groups on PIBSA as a function of the reaction time in a B2.5 blend. Premixing performed at 80°C.

to 280 min where a conversion of 10% is reached; at longer times, the process slows down considerably and the maximum conversion is attained after about 1000 min. The very slow reaction rate compared with that of low molecular weight analogs (i.e., propanol and MA<sup>16</sup>) might be ascribed to the fact that the system under investigation is heterogeneous. Under such conditions, the rate-limiting step is the diffusion of the SA end groups toward the surface of the rubbery domains. Moreover, the limited yield is likely due to the fact that two different hydroxyl functionalities are present as UP end groups, namely, primary and secondary OH groups deriving from the polycondensation of the starting monomers isopropylene glycol and MA.

It is known from the literature<sup>15</sup> that secondary alcohols do not react with MA in the absence of suitable catalytic systems; thus, in our case, only a limited number of OH end groups, i.e., the primary ones, are able to interact chemically with MA.

The diblock copolymer formed upon reaction of the reactive end groups of PIB and of UP is likely to act as an emulsifying agent in the blend, thus improving the dispersion of the rubbery component in the matrix before cure and enhancing the interfacial adhesion after the crosslinking process. As will be shown in the next paragraphs, interesting results in terms of toughness and morphology may be achieved even with limited yields of such a copolymer.

### Mechanical and Fracture Properties

The Young's modulus,  $E$ , of the neat UP and of the various blend compositions investigated was determined in the flexural mode at ambient and at a crosshead speed of 1 mm/min, using the equation<sup>17</sup>

$$E = \frac{L^3P}{4dWB^3} \quad (5)$$

**Table II** Elastic Modulus ( $E$ ) and Compressive Yield Stress ( $\sigma_{y,c}$ ) of the UP/Rubber Blends

Code	$E$ (N/mm <sup>2</sup> )	$\sigma_{y,c}$ (MPa)
UP	2300	85.0
B0	2000	74.0
B1.5	2050	73.5
B2.5	2050	73.2
B2.5*	2000	72.1

\* Premixed 12 h before curing.

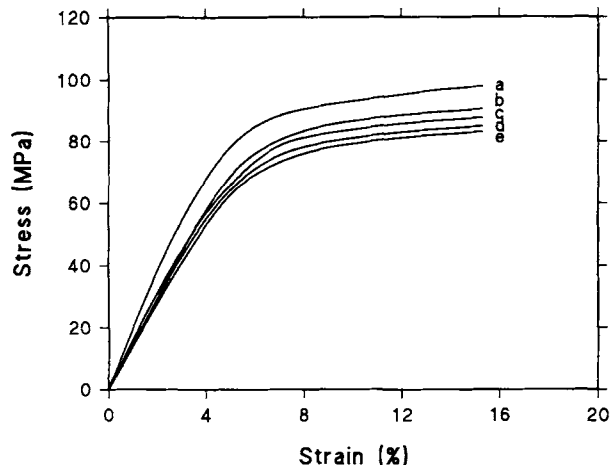


**Figure 7** Compressive stress-strain curves at ambient temperature and at 1 mm/min, (a) pure UP resin, (b) B0 blend, (c) B1.5 blend, (d) B2.5 blend, and (e) B2.5\* blend.

where  $d$  is the displacement;  $P$ , the load at the displacement  $d$ ;  $L$ , the span; and  $W$  and  $B$ , the width and the thickness of the specimen, respectively.

The  $E$  values are reported in Table II; as expected, for all the materials tested, a decrease of modulus, compared with that of the plain resin, is observed. Moreover, such an effect is independent of the type of rubber used as well as of its grafting degree.

To predict large strain properties, the yielding behavior of all the investigated blends was examined under uniaxial compression mode. Typical stress-strain curves obtained at the same loading rate and temperature as for the Young's modulus are shown in Figure 7.

It can be observed that, when loaded in compression, all the samples yield and flow, contrary to what happens in tension,<sup>8</sup> where they exhibit a completely brittle behavior. For convenience, all the stress-strain curves have been reported up to 16% deformation, although some samples were found to deform to strains exceeding 20%. The compressive yield stress,  $\sigma_{c,y}$ , was evaluated according to the following equation:

$$\sigma_{c,y} = \frac{P}{A_0} (1 - \epsilon) \quad (6)$$

where  $P$  is the load;  $A_0$ , the initial cross-sectional area of the specimen; and  $\epsilon$ , the specimen strain. The values of  $\sigma_{c,y}$  are reported in Table II; the same behavior as that found for the Young's modulus is observed. The decrease of  $\sigma_{c,y}$  upon rubber addition is a direct consequence of the lower shear modulus

of the rubbery phase compared with that of the UP matrix, which prevents the rubbery domains from supporting a significant amount of the applied stress.

The fracture behavior of both the unmodified and the rubber-modified resins was examined at low and high strain rates. For both plain UP and UP/rubber blends at a low deformation rate (1 mm/mm), the crack propagation was stable-brittle, with no evidence of a stick-slip propagation.<sup>18</sup> The critical stress intensity factor,  $K_c$ , determined from the load-displacement curves using eq. (1), is reported in Figure 8. In the same figure are also reported the values of  $K_c$  determined under impact conditions.

The UP resin exhibits low values of  $K_c$  in both test conditions, according to its poor crack resistance. Similar results are observed for the blend containing unmodified PIB as a rubbery phase. In contrast, the blends containing PIBSA display a marked improvement in fracture toughness.

An analogous trend is observed when the fracture data are expressed in term of the parameter,  $G_c$ , (see Fig. 9). The observed improvement of  $K_c$  and  $G_c$  is found to be dependent on two factors:

1. The grafting degree of PIBSA.
2. The time period during which the UP/PIBSA mixture was allowed to react prior to the curing process (premixing step).

In particular, we observed an increase in the  $K_c$  and  $G_c$  parameters with increasing the grafting degree; moreover, for the same grafting degree of 2.5 by weight, a further enhancement of toughness is achieved by increasing the premixing time from 60 min to 12 h.

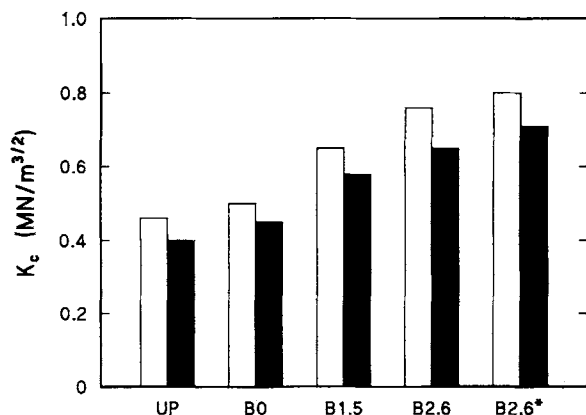


**Figure 8** Critical stress intensity factor  $K_c$  for the various investigated blend compositions: (□) low-speed tests; (■) high-speed tests.

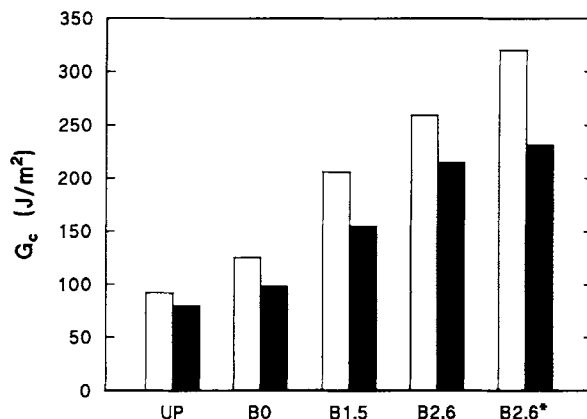


**Figure 9** Critical strain energy release rate  $G_c$  for the various investigated blend compositions: (□) low-speed tests; (■) high-speed tests.

The effect of grafting degree on the toughness parameters may be ascribed to the formation of a UP/PIB block copolymer, which, acting as an emulsifier, reduces the particle size of the rubbery domains and firmly bonds the two phases together once the curing reaction has occurred; the higher the grafting degree of the rubber, the higher the concentration of the emulsifier in the blend. Analogously, the effect of the premixing time can be accounted for by considering that the conversion of MA and, hence, the amount of the diblock copolymer formed, increases going from 60 min to 12 h (see Fig. 6).

From the viewpoint of the deformation mechanism, as will be shown in the subsequent paragraph, the above enhancement of toughness can be ascribed to the formation of multiple but localized shear deformation bands in the matrix induced by the presence of rubber particles which act as stress concentrators. As the size of the rubber particles decreases and the size distribution gets more homogeneous, the mechanism of induction of plastic deformation in the matrix becomes more efficient.<sup>19</sup>

A further parameter which plays a key role in enhancing the toughness is the interfacial adhesion.<sup>20</sup> When good adhesion is realized, the rubber domains are able to act as load-bearing components due to the continuity of the structure. Thus, extensive shear deformation may occur near the crack tip which can absorb a large amount of energy before the final fracture. This process is strongly reduced when there is poor or no adhesion at the particle-matrix interface.

It has been shown that, for relatively brittle polymers, the extent and shape of the localized plastic



**Table III Estimation of the Plastic Zone Size Using Dugdale ( $R$ ) and Irwin ( $r_p$ ) Models**

Code	$R$ ( $\mu\text{m}$ )	$r_p$ ( $\mu\text{m}$ )
UP	19.6	2.6
B0	32.8	4.4
B1.5	55.0	7.4
B2.5	73.3	9.9
B2.5*	88.4	12.0

\* Premixed 12 h before curing.

deformation ahead of a crack tip can be successfully described using the models developed by Dugdale<sup>21</sup> and Irwin.<sup>22</sup> For the Dugdale’s model, the size of the plastic zone  $R$  is given by

$$R = \frac{\pi}{8} \left( \frac{K_c}{\sigma_{t,y}} \right)^2 \quad (7)$$

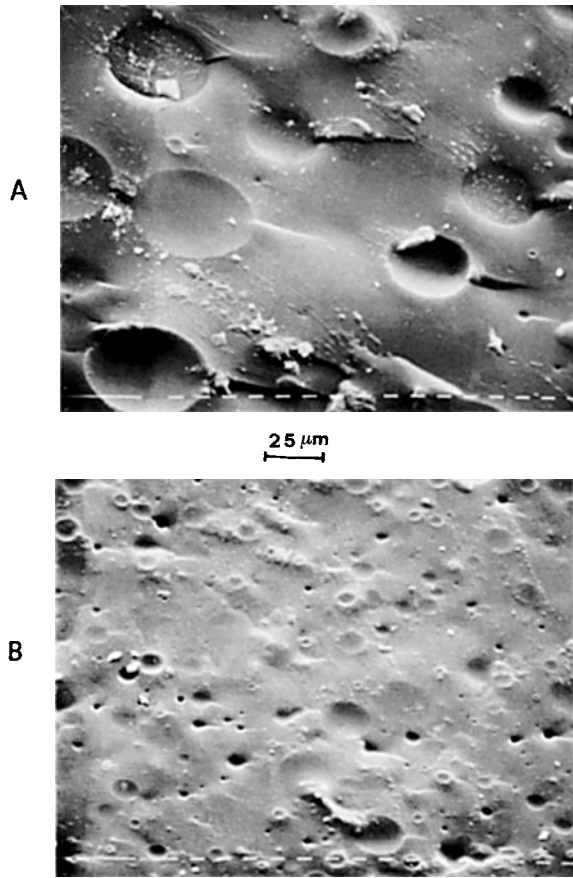


**Figure 10** SEM micrographs of the fracture surfaces of samples broken at low deformation rate: (A) B0 blend; (B) B1.5 blend.

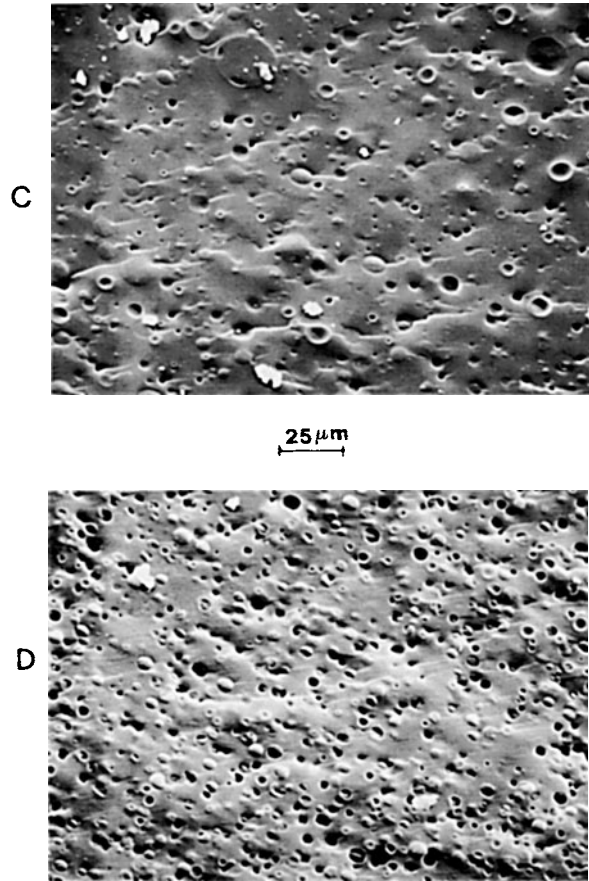


**Figure 11** SEM micrographs of the fracture surfaces of samples broken at low deformation rate: (C) B2.5 blend; (D) B2.5\* blend.

where  $\sigma_{t,y}$  is the tensile yield stress. Similarly, for the Irwin model, the size of the plastic zone  $r_p$  may be evaluated, for the plain strain case by

$$r_p = \frac{1}{6\pi} \left( \frac{K_c}{\sigma_{t,y}} \right)^2 \quad (8)$$

Comparison of eq. (7) and eq. (8) reveals that the Dugdale’s model predicts a larger extent of plasticity than does the Irwin model. However, both equations predict that the plastic size zone is proportional to  $(K_c/\sigma_{t,y})^2$ .

The  $R$  and  $r_p$  values, calculated according to eq. (7) and eq. (8), are reported in Table III. The tensile yield stress values were obtained from the uniaxial compression tests assuming the ratio  $\sigma_{t,y}/\sigma_{c,y}$  to be equal to 0.75.<sup>5,23</sup> Both the  $R$  and  $r_p$  parameters increase by increasing the grafting degree of the PIB rubber and, for the same grafting degree, by increasing the premixing time. These results further con-

firm that the efficiency of PIB as a toughening agent depends on the amount of the PIB/UP block copolymer formed during processing.

### Morphological Analysis

Scanning electron micrographs of rubber-modified UP blends fractured at low deformation rate are reported in Figures 10 and 11. All the fracture surfaces are characterized by a morphology in which the rubber is segregated into spherical shaped domains dispersed in the UP matrix. In particular, the UP/PIB blend [Fig. 10(A)] shows few large cavities with a diameter ranging from 80 to 100  $\mu\text{m}$  corresponding to the positions of the rubber domains pulled off during fracture. Moreover, the UP matrix around the cavities appears rather flat, indicating its very limited plastic deformation.

When PIB is replaced with PIBSA [Figs. 10(B)

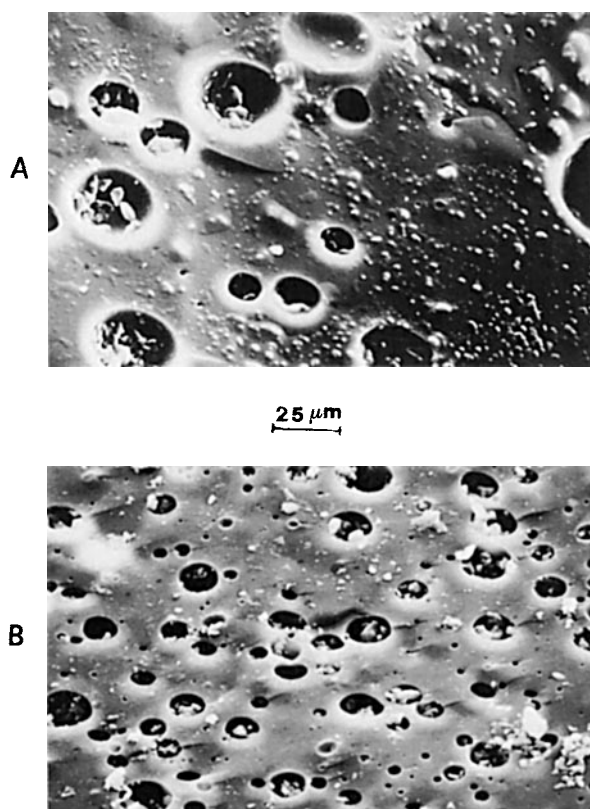


**Figure 12** SEM micrographs of the fracture surfaces of samples broken at low deformation rate and subsequently etched with  $\text{CHCl}_3$  vapors; (A) B0 blend; (B) B1.5 blend.

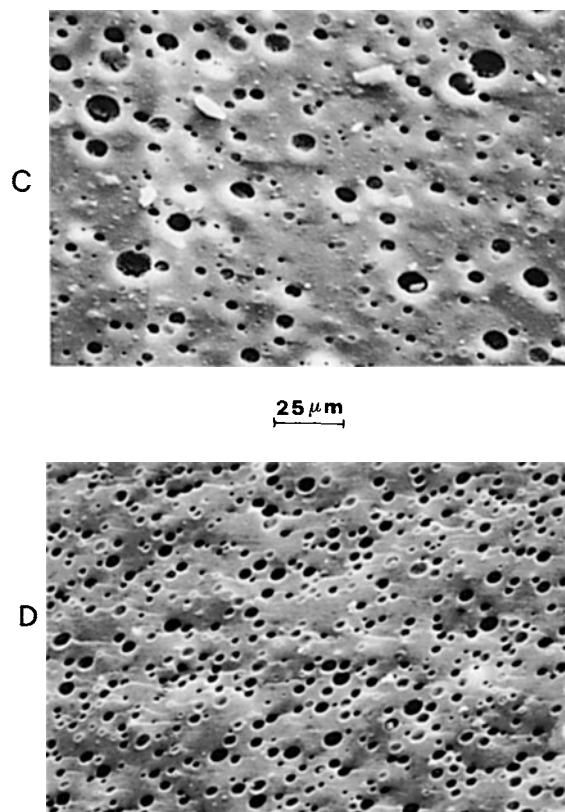


**Figure 13** SEM micrographs of the fracture surfaces of samples broken at low deformation rate and subsequently etched with  $\text{CHCl}_3$  vapors: (C) B2.5 blend; (D) B2.5\* blend.

and 11], strong variations in the overall fracture morphology are observed: In general, a substantial reduction of the particle size is brought about by the PIB functionalization, as well as a more homogeneous distribution of the particle sizes. The fracture surfaces of these samples also display evidence of shear deformation of the UP matrix around the rubber particles. This phenomenon, which confirms the toughening mechanism advanced in the previous paragraph, is more evident in the blends with the higher grafting degree (see Fig. 11).

To put the above observations on a more quantitative basis, we performed a complete image analysis of the fracture surfaces. To obtain meaningful results by this approach, it is necessary to achieve good contrast among the phases. To this end, an etching treatment of the samples was performed by  $\text{CHCl}_3$  vapors so as to completely remove the rubber particles from the fracture surfaces. The analysis was carried out on a large number of images (more

than 10); examples of the etched surfaces used are shown in Figures 12 and 13.

The frequency vs. particle-size histogram of the B0 blend [see Fig. 14(A)] shows a very broad distribution of sizes with an average diameter  $\bar{D}$  of 75  $\mu\text{m}$  and a standard deviation,  $\sigma$ , of 36.0. Conversely, when PIBSA is used [see Figs. 14(B) and 15], the average particle size decreases by about one order of magnitude and the distribution becomes substantially narrower. The  $\bar{D}$  and  $\sigma$  values of the various investigated blends are collectively reported in Table IV.

The above effects are found to depend on the grafting degree (GD) of PIBSA: In fact, in going from a GD of 1.5 to a GD of 2.5,  $\bar{D}$  decreases from 14.0 to 8.0 and  $\sigma$  goes from 7.6 to 4.7. It is worth noting that the blends having the same GD of the rubber, but prepared with different premixing times, exhibit the same values of  $\bar{D}$ , but  $\sigma$  goes from 4.7 to 3.5 by increasing the premixing time. Thus, the net effect of this processing step is simply to induce a

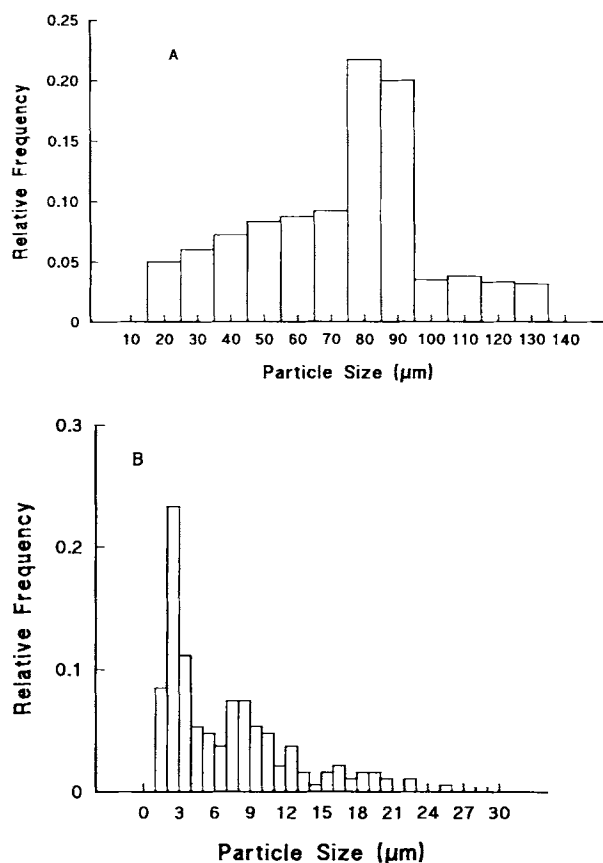


Figure 14 Particle-size distribution: (A) B0 blend; (B) B1.5 blend.

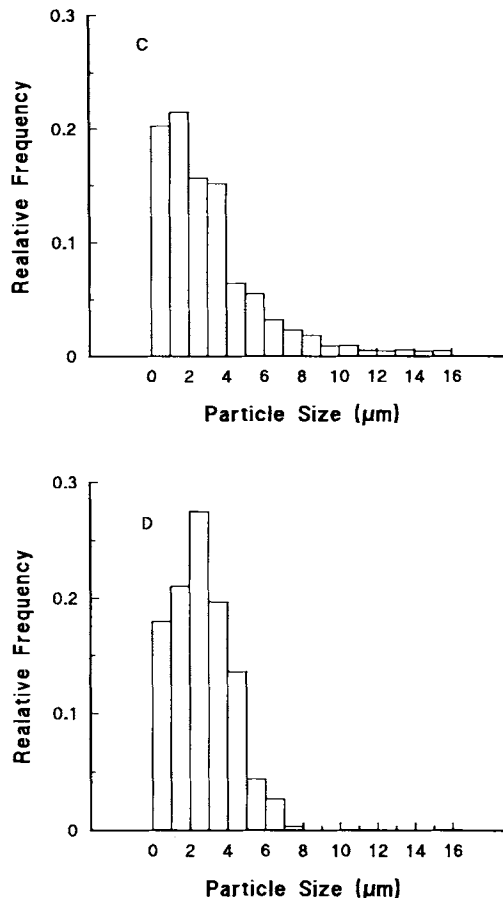


Figure 15 Particle-size distribution: (C) B2.5 blend; (D) B2.5\* blend.

more homogeneous distribution of the rubber particles within the matrix, while the average diameter remains unaffected. In turn, the narrowing of the particle-size distribution produces a limited effect on the toughening properties of the blend.

The whole of the experimental results described

Table IV Average Diameter,  $\bar{D}$ , and Standard Deviation,  $\sigma$ , of the Rubber Domains in the Various Investigated Blends

Code	$\bar{D}$ ( $\mu\text{m}$ )	$\sigma$
B0	75.0	36.0
B1.5	14.0	7.6
B2.5	8.0	4.7
B2.5*	8.0	3.5

\* Premixed 12 h before curing.

herein indicate that, in order to achieve a significant toughening effect, it is not necessary that the total amount of rubber introduced in the blend is reactive toward the thermosetting matrix. Even with conversion of the reactive functionalities as low as those obtained after 1 h of premixing (see Fig. 6), a material with interesting toughening properties can be obtained. This, in turn, implies that the amount of interfacial agent needed to produce a morphology suitable to achieve the desired properties is rather low. This same behavior has been found also in the toughening of thermoplastic matrices such as polyamides.<sup>24</sup> Thus, an alternative approach to toughen thermosetting matrices which would avoid the very long and impractical premixing step is to prepare by a separate process the compatibilizing copolymer and to add small amounts of it to the unmodified liquid rubber prior to blending. Work is in progress in our laboratories to optimize this type of process.

## CONCLUSIONS

A polyisobutene rubber has been modified by grafting succinic anhydride onto its end groups. The process, carried out in solution by means of an organic radical initiator, yielded a maximum grafting degree of 2.5% by weight. The reaction product was characterized by FTIR spectroscopy to determine its grafting degree as well as the preferential site of attack of the MA moiety onto the rubber.

It was shown that the vinyl end groups disappeared completely upon maleation of the rubber, thus suggesting a likely reaction mechanism. The PIBSA rubber thus prepared was used as a toughening agent in UP-based blends. Kinetic measurements performed by FTIR spectroscopy showed that the MA groups of the rubber are able to react with the hydroxyl end groups of the polyester prepolymers forming a diblock copolymer of the type UP/PIB. However, due to the heterogeneity of the reactive mixture, the reaction rate was very slow and the final yield did not exceed 15%.

The mechanical and the fracture properties of a series of blends were investigated. The modulus and the yield stress decreased upon addition of the second component irrespective of the type and of the grafting degree of the rubber.

Fracture measurements performed at high and low rates of deformation demonstrated a substantial increase of toughness when PIBSA was used as modifier. In particular, the best results were achieved with the highest grafting degree of the rubber and

when the components were premixed for 12 h prior to the curing process. These results were interpreted on the basis of the role played by the UP/PIB copolymer as interfacial agent.

The morphological analysis of the fractured surfaces revealed a drastic reduction of the size of the rubbery domains when PIBSA is used in place of plain PIB as second component. Moreover, image analysis showed that the reduction of particle size is accompanied by a considerable narrowing of the particle-size distribution. In agreement with the fracture results, both these effects were enhanced by increasing the grafting degree.

In the light of the above results, it can be concluded that, in order to achieve a satisfactory level of toughening, it is sufficient to form *in situ* or to add during processing a limited amount of a copolymer which can act as a compatibilizing agent.

Thanks are due to Mr. V. Di Liello and Mr. A. Lahoz for their technical assistance in performing the mechanical and fracture measurements and to Mr. G. Orsello for his help in carrying out the morphological analysis. This work has been partially supported by C.N.R. "Progetto Finalizzato Chimica Fine II."

## REFERENCES

1. C. K. Riew and J. K. Gillham, Eds., in *Rubber Modified Thermoset Resins*, Adv. Chem. Sci., American Chemical Society, Washington, DC, 1984, p. 208.
2. C. K. Riew, E. H. Rowe, and A. R. Siebert, in *Toughness and Brittleness of Plastics*, R. D. Deanin and A. M. Crugnola, Eds., American Chemical Society, Washington, DC, 1976, p. 326.
3. A. J. Kinloch and R. J. Young, *Fracture Behavior of Polymers*, Applied Science, London, 1983.
4. A. F. Yee and R. A. Pearson, *J. Mater. Sci.*, **21**, 2462 (1986).
5. A. J. Kinloch, S. J. Shaw, and D. L. Hunston, *Polymer*, **24**, 1355 (1983).
6. J. A. Crosbie and M. G. Phillips, *J. Mater. Sci.*, **20**, 563 (1985).
7. E. Martuscelli, P. Musto, G. Ragosta, G. Scarinzi, and E. Bertotti, *J. Polym. Sci.*, **31**, 619 (1993).
8. J. C. Williams, *Fracture Mechanics of Polymers*, Wiley, New York, 1984.
9. W. F. Brown and J. Srawley, ASTM STP410, American Society for Testing and Materials, Philadelphia, 1966, p. 13.
10. E. Plati and J. G. Williams, *Polym. Eng. Sci.*, **15**, 470 (1975).
11. M. Abbate, V. Di Liello, E. Martuscelli, P. Musto, G. Ragosta, and G. Scarinzi, *Polymer*, **33**, 2940 (1992).

12. R. Greco, G. Maglio, P. Musto, and G. Scarinzi, *J. Appl. Polym. Sci.*, **37**, 777 (1989).
13. R. Greco, G. Maglio, P. Musto, and F. Riva, *J. Appl. Polym. Sci.*, **37**, 789 (1989).
14. B. C. Trivedi and B. M. Culbertson, *Maleic Anhydride*, Plenum Press, New York, 1982, pp. 466-472.
15. J. Sheng, X. L. Lu, and K. D. Yao, *J. Macromol. Sci.*, A 27(2), 167 (1990).
16. B. C. Trivedi and B. M. Culbertson, *Maleic Anhydride*, Plenum Press, New York, 1982, pp. 78-80.
17. S. Yamini and R. J. Young, *J. Mater. Sci.*, **15**, 1814 (1980).
18. A. J. Kinloch, S. J. Shaw, D. A. Tod, and D. L. Hunston, *Polymer*, **24**, 1341 (1983).
19. C. B. Bucknall, *Toughened Plastics*, Applied Science, London, 1977.
20. A. F. Yee and R. A. Pearson, *Fractography and Failure Mechanisms in Polymers and Composites*, A. C. Roulin-Moloney, Ed., Elsevier, London, 1989.
21. D. S. Dugdale, *J. Mech. Phys. Solids*, **8**, 100 (1960).
22. G. R. Irwin, *Appl. Mater. Res.*, **3**, 65 (1964).
23. J. N. Sultan and M. McGany, *J. Polym. Eng. Sci.*, **13**, 29 (1973).
24. R. Greco, M. Malinconico, E. Martuscelli, G. Ragosta, and G. Scarinzi, *Polymer*, **29**, 1418 (1988).

*Received February 23, 1995*

*Accepted April 18, 1995*